Published in final edited form as:
*Bioconjug Chem*. 2012 May 16; 23(5): 1029–1039. doi:10.1021/bc300037w.

# Comparison of $^{64}$Cu-complexing bifunctional chelators for radioimmunoconjugation: labeling efficiency, specific activity and *in vitro/in vivo* stability

**Maggie S. Cooper**[‡,*], **Michelle T. Ma**[†], **Kavitha Sunassee**[‡], **Karen P. Shaw**[‡], **Jennifer D. Williams**[‡], **Rowena L. Paul**[‡], **Paul S. Donnelly**[†], and **Philip J. Blower**[‡]

[‡]King's College London, Division of Imaging Sciences and Biomedical Engineering, 4th Floor Lambeth Wing, St. Thomas' Hospital, SE1 7EH, London

[†]School of Chemistry and Bio21 Molecular Science and Biotechnology Institute, University of Melbourne, Parkville, Melbourne, Victoria, 3010, Australia

## Abstract

High radiolabeling efficiency, preferably to high specific activity, and good stability of the radioimmunoconjugate are essential features for a successful immunoconjugate for imaging or therapy. In this study, the radiolabeling efficiency, *in vitro* stability and biodistribution of immunoconjugates with eight different bifunctional chelators labeled with $^{64}$Cu were compared. The anti-CD20 antibody, rituximab, was conjugated to four macrocyclic bifunctional chelators (*p*-SCN-Bn-DOTA, *p*-SCN-Bn-Oxo-DO3A, *p*-SCN-NOTA and *p*-SCN-PCTA), three DTPA derivatives (*p*-SCN-Bn-DTPA, *p*-SCN-CHX-A"-DTPA and ITC-2B3M-DTPA) and a macrobicyclic hexamine ("sarcophagine") chelator (sar-$CO_2$H) = (1-$NH_2$-8-NHCO($CH_2$)$_3$$CO_2$H)sar where sar = sarcophagine = 3,6,10,13,16,19-hexaazabicyclo[6.6.6]icosane). Radiolabeling efficiency under various conditions, *in vitro* stability in serum at 37°C and *in vivo* biodistribution and imaging in normal mice over 48 h were studied. All chelators except sar-$CO_2$H were conjugated to rituximab by thiourea bond formation with an average of 4.9 +/− 0.9 chelators per antibody molecule. Sar-$CO_2$H was conjugated to rituximab by amide bond formation with 0.5 chelators per antibody molecule. Efficiencies of $^{64}$Cu radiolabeling were dependent on the concentration of immunoconjugate. Notably, the $^{64}$Cu-NOTA-rituximab conjugate demonstrated highest radiochemical yield (95%) under very dilute conditions (31 nM NOTA-rituximab conjugate). Similarly, sar-CO-rituximab, containing 1/10$^{th}$ the number of chelators per antibody compared to other conjugates retained high labeling efficiency (98 %) at an antibody concentration of 250 nM. In contrast to the radioimmunoconjugates containing DTPA derivatives, which demonstrated poor serum stability, all macrocyclic radioimmunoconjugates were very stable in serum with <6 % dissociation of $^{64}$Cu over 48 h. *In vivo* biodistribution profiles in normal female Balb/C mice were similar for all the macrocyclic radioimmunoconjugates with most of the activity remaining in the blood pool up to 48 h. Whilst

[*]Corresponding Author: King's College London Division of Imaging Sciences and Biomedical Engineering 4th Floor Lambeth Wing St. Thomas' Hospital London, UK SE1 7EH Phone: +44 (0)20 7188 8376 Margaret.s.cooper@kcl.ac.uk.

**Supporting Information Available:** Experimental data regarding radiolabeling efficiencies of each immunoconjugate under increasingly dilute conditions, bifunctional chelator to antibody ratio determination, PET images for all radioimmunoconjugates and HPLC radiochromatograms of radioimmunoconjguates. This material is available free of charge via the Internet at http://pubs.acs.org.


Europe PMC Funders Author Manuscripts

all the macrocyclic bifunctional chelators are suitable for molecular imaging using $^{64}$Cu-labeled antibody conjugates, NOTA and sar-$CO_2$H show significant advantages over the others in that they can be radiolabeled rapidly at room temperature, under dilute conditions resulting in high specific activity.



Europe PMC Funders Author Manuscripts

## Introduction

Radioimmunoconjugates comprising antibodies attached to a bifunctional chelator (BFC) and radiolabeled with a metallic radioisotope provide an excellent way of delivering radioactivity selectively to a tumor target. An appropriate choice of both antibody and radioisotope is essential whether the purpose is imaging or therapy[1].

$^{64}$Cu ($t_{1/2}$ = 12.7h), with both $\beta^+$ and $\beta^-$ emissions, allows for both PET imaging and radionuclide therapy, and $^{64}$Cu labeled antibodies have attracted considerable interest in the field of targeted radionuclide therapy and diagnosis. In addition, copper has several other medically relevant isotopes ($^{60}$Cu, $^{61}$Cu, $^{62}$Cu and $^{67}$Cu) that are potentially useful for either diagnosis or therapy[2, 3]. Although direct labeling approaches for labeling antibodies with $^{64}$Cu have been proposed[4], indirect labeling using a BFC is the preferred method to control stability of the $^{64}$Cu-antibody complex formed. Improvements in chelators and radiolabeling methods will provide radioimmunoconjugates that are better able to target these copper isotopes to the tumor site.

Numerous chelators have been reported for complexing copper[5-16] and several of these have been functionalized to allow attachment to antibodies[17-34] and are now commercially available. The choice of antibody/BFC combination will affect efficacy as an imaging or therapy agent. Whilst some side-by-side standardized comparisons of chelators conjugated to antibodies have previously been described[18-23], a comparative investigation of radiolabeling efficiencies for the most readily available bifunctional chelators has not been reported. Moreover, many of the reported chelators have been evaluated under labeling conditions that are not sufficiently exacting to demonstrate superiority over others or real practical utility as high quality radiopharmaceutical components.

Several key factors must be considered when optimizing an immunoconjugate for its designed purpose. The method of conjugation must not result in degradation of the antibody, and radiolabeling should be rapid and result in high specific activity. *In vivo*, the radioimmunoconjugate must provide sufficient ‘target-to-background’ ratio to provide high quality diagnostic images or target-selective therapy, in turn requiring high *in vivo* integrity as loss of copper from the BFC will cause accumulation in non-target tissues, such as the liver. The radiolabeling should be rapid and easily performed at low antibody concentration to achieve high specific activity.

The choice of BFC can influence the biodistribution of radioactivity *in vivo*[18-24, 35-41], with biodistribution related to the *in vivo* stability of the $^{64}Cu^{2+}$-BFC complex. Generally high liver activity is assumed to be indicative of instability of the $^{64}Cu^{2+}$-BFC complex *in vivo*. Transchelation of $^{64}$Cu to serum components (e.g. albumin[18, 42]) or in the liver to ceruloplasmin[43], metallothionein or superoxide dismutase, may occur[44].

In this study, we compared six commercially available isothiocyanatobenzyl BFCs (see Fig. 1): *S*-2-(4-isothiocyanatobenzyl)-1,4,7-triazacyclononane-1,4,7-triacetic acid (*p*-SCN-Bn-NOTA); 2-(4-isothiocyanatobenzyl)-1,4,7,10-tetraazacyclododecane-1,4,7,10-tetraacetic acid (*p*-SCN-Bn-DOTA); 1-oxa-4,7,1-tetraazacyclododecane-5-*S*-(4-isothiocyanatobenzyl)-4,7,10-triacetic acid (*p*-SCN-Bn-oxo-DO3A); 3,6,9,15-tetraazabicyclo[9.3.1]- pentadeca-1(15),11,13-triene-4-*S*-(4-isothiocyanatobenzyl)-3,6,9-triacetic acid (*p*-SCN-Bn-PCTA); 2-(4-isothiocyanatobenzyl)-diethylenetriaminepentaacetic acid (*p*-SCN-Bn-DTPA); N-[*R*-2-amino-3-(*p*-isothiocyanato-phenyl)propyl]-trans-(*S*,*S*)-cyclohexane-1,2-diamine-*N*,*N*,*N'*,*N"*,*N"*-pentaacetic acid (CHX-A"-DTPA). We also included 2-benzyl-3-methylisothiocyanato-diethylenetriaminepentaaceticacid (2B3M-ITC-DTPA) and a sarcophagine ligand, (1-$NH_2$-8-$NHCO(CH_2)_3CO_2H$)sar where sar = sarcophagine = 3,6,10,13,16,19-hexaazabicyclo[6.6.6]icosane (sar-$CO_2H$)[45, 46]. Encapsulating hexaamine sarcophagine ligands, first prepared by Sargeson and co-workers[47-51], form extraordinary stable complexes with copper(II) and benefit from rapid complexation rates[52, 53]. Methods have been developed to introduce reactive functional groups to the ligand framework[54-56], to allow the ligands to be conjugated to peptides and antibodies with a goal of synthesizing copper radiopharmaceuticals that benefit from the special properties of sarcophagine ligands[21, 45, 46, 57-61]. Each BFC was conjugated to the anti-CD20 antibody, rituximab, as a model antibody with clinical utility. We assessed radiolabeling efficiency under increasing dilution, stability in serum and *in vivo* biodistribution in normal female Balb/C mice to identify the best BFC for radioimmunotherapy and diagnostic studies with copper radioisotopes.

## Materials and methods

### General

Chemicals and reagents were obtained from Sigma-Aldrich (Dorset, UK) unless otherwise specified. The highest available purity (lowest metal ion-containing) chemicals were used. Sterile water for injection, used to prepare buffers, was obtained from Baxter Healthcare (Newbury, UK). G-25 (Sephadex) size exclusion columns were purchased from GE Healthcare (Chalfont St. Giles, UK) and washed with 0.1 M ammonium acetate solution, pH 6. Vivaspin 2 ultracentrifugation tubes were purchased from Sartorius (Epsom, UK). BFCs were purchased from Macrocyclics, Inc. (Dallas, TX) except for 2B3M-ITC-DTPA, which was a gift from Dr. Kim Orchard (Haematology Department, Southampton General Hospital) and sar-$CO_2H$, which was prepared as previously described[45, 46]. Rituximab (MabThera, Roche) was obtained as a 10 mg/ml solution from the Pharmacy Department at Guy's and St. Thomas' NHS Trust, London. Male AB type human serum was obtained from Sigma (product H4522, this serum contains sodium citrate which is added as part of the preparation process). High-performance liquid chromatography (HPLC) analysis was carried out on an Agilent 1200 series system with in-line UV (280 nm) and gamma detector (Flow-Count, LabLogic). Instant thin layer chromatography strips (ITLC-SA) were obtained from Varian Medical Systems UK, Ltd. (Crawley, UK).

### Antibody conjugation of p-SCN-Bn-derivatised BFCs

To rituximab (10 mg, 1 mL) was added 50 mM EDTA (50 μL) to complex any free trace metal ion. The antibody was buffer exchanged and concentrated to approximately 10 mg/mL in 0.1 M HEPES buffer, pH 8.9 in Vivaspin 2 ultracentrifugation tubes. The antibody was transferred to a cryovial (Nalgene) and conjugation to the BFCs was carried out as previously described with slight modification[62]. A 40-fold molar excess of each BFC over antibody in DMSO (40 μL) was added to the antibody in 0.1 M HEPES buffer, pH 8.9. Conjugation was allowed to proceed at room temperature for 2 h and continued overnight at 2 - 8°C. Excess chelator was removed initially by G25 Sephadex size exclusion purification (PD-10 column). The immunoconjugate was eluted with 0.1 M ammonium acetate solution, pH 6. Fractions containing the immunoconjugate were combined and then further purified by centrifugal ultrafiltration (Vivaspin 2). The volume was reduced to approximately 0.5 mL during centrifugation. After each centrifugation step, the immunoconjugate was resuspended and diluted to 2 mL with 0.1 M ammonium acetate solution, pH 6. The immunoconjugate was finally concentrated to 2 mg/mL in 0.1 M ammonium acetate solution, pH 6.

### Antibody conjugation of sar-$CO_2H$

To rituximab (10 mg, 1 mL) was added 50 mM EDTA (50 μL) to complex any free trace metal ion. The antibody was buffer exchanged and concentrated to approximately 10 mg/mL in 0.1 M phosphate buffer, pH 7, in Vivaspin 2 ultracentrifugation tubes. The antibody was transferred to a cryovial (Nalgene).

The NHS ester of sar-$CO_2$ was prepared by first mixing sulfo-*N*-hydroxysuccinimide (4 mg) in 0.1 M phosphate buffer, pH 7 (40 μL) with sar-$CO_2$ (4.7 mg) in 0.1 M phosphate buffer, pH 7 (80 μL) and then adding 1-ethyl-3-(3-dimethylaminopropyl)carbodiimide (1.5 mg) in 0.1 M phosphate buffer, pH 7 (15 μL). This solution (32 μL) was added to the antibody and the mixture left at room temperature (21 °C) for 90 min. The immunoconjugate was purified as detailed above.

### $^{64}$Cu production

$^{64}$Cu was prepared by $^{64}$Ni(p,n)$^{64}$Cu nuclear reaction on a CTI RDS 112 11 MeV cyclotron. The irradiated $^{64}$Ni (10 mg) was dissolved from the gold target on which it was electroplated in minimal concentrated hydrochloric acid (100-150 μl) and $^{64}$Cu purified to yield $^{64}CuCl_2$ by loading onto an anion exchange column (Biorad AG1-X8 resin). Excess $^{64}$Ni was removed by elution in 9 M HCl. 6 M HCl was then used to reduce the pH before elution of the $^{64}Cu^{2+}$ in 0.1 M HCl (see Figure 2). Fraction 9 (the fraction after the main $^{64}$Cu elution) was used because fraction 8 consistently gave poorer labeling and more aggregation and precipitation of the antibody even when the pH of the $^{64}$Cu solution was adjusted adequately. Fraction 9 was diluted with an equal volume of 1 M ammonium acetate solution bringing the pH to 6. This solution contains approx. 0.5 M chloride and 0.5 M acetate.

### Radiolabeling

Typically $^{64}$Cu solution prepared as above (37 MBq, 120 μL) was added to 240 μg (120 μL) immunoconjugate solution prepared as above and the resulting solution incubated at room

temperature for 20 min. In the case of DOTA-rituximab, the solution was heated at 37°C for 90 min in light of literature precedent, however, it was subsequently found that the radiolabeling proceeded adequately at room temperature in 20 min (see below). Analysis was performed by instant thin layer chromatography using ITLC-SA (Varian) with a mobile phase of 0.1M citrate buffer (pH 5) and by size exclusion HPLC using a BioSep SEC-S-2000 column (Phenomenex, Macclesfield, UK) with an isocratic mobile phase of 0.1M phosphate buffer containing 2 mM EDTA, pH 7 and a flow rate of 1 mL/min. The retention time of the immunoconjugate was typically 7 min and that of the unbound $^{64}$Cu impurities was approximately 11 min.

### Radiolabeling of DOTA-Rituximab under different conditions

To each of three samples of DOTA-rituximab (20 μL, 40 μg) was added $^{64}$Cu solution (15 MBq, 20 μL). One sample was incubated at 4-8°C for 20 min, another at ambient temperature (25°C) for 20 min and a third at 37°C for 20 min. Following incubation, a 20 μL sample was analysed by HPLC and a 2000-fold molar excess of EDTA (50 mM, 5 μL) was added to the remaining solution. The samples were left at room temperature for 40 min then analyzed by HPLC.

### BFC to antibody ratio

The average number of chelators per antibody was assessed using a modification of the method of Meares *et al.*[63, 64] using a mixture of $^{64}$Cu and cold copper rather than cobalt. A small amount of $^{64}$Cu solution was added to a known concentration of copper(II) chloride solution to give a 0.25 mM $Cu^{2+}$ solution. To the immunoconjugate ($1.25 \times 10^{-10}$ moles) were added increasing ratios of copper ($1.25 \times 10^{-9}$ – $1.25 \times 10^{-8}$ moles) and the total volume of the reaction was adjusted to 100 μL by addition of 0.1 M ammonium acetate solution, pH 6. The solution was incubated at room temperature for 20 min (or at 37°C for 90 min in the case of DOTA-rituximab) after which time a solution of 50 mM EDTA (2 μL, approximately 1000:1 molar ratio of EDTA:immunonconjugate) was added to complex any unbound copper. Five min after addition of EDTA, the reaction solution was analyzed on ITLC-SA (0.75 × 9 cm) with the origin at 1 cm from the bottom of the strip and the solvent front at 8 cm. 1.5 μL of the radiolabeled immunoconjugate was spotted at the origin and the strip was allowed to air dry and then developed in 0.1 M citrate buffer, pH 5. The strip was cut in half and the radioactivity in each half counted using a gamma counter. It had previously been determined from visualizing the strip on a PhosphorImager that EDTA-complexed copper moved to the upper half of the TLC strip and the radiolabeled antibody remained at the origin. The labeling efficiency at different copper to immunoconjugate ratios was calculated and from this the number of moles of copper specifically bound at each ratio was determined for each immunoconjugate. Knowing the moles of immunoconjugate used initially, the number of chelators per antibody was determined (see supplementary data).

### Radiolabeling dilution assay

Serial dilutions of immunoconjugates were prepared in 0.1 M ammonium acetate solution, pH 6, and $^{64}$Cu solution (~1.3 MBq, approx 1 – 5 μL) added to give immunoconjugate concentrations of 500 nM – 15.6 nM in 100 μL. Mixtures were incubated at room

temperature for 20 min (or at 37°C for 90 min in the case of DOTA-rituximab) and 50 mM EDTA solution (2 μL, a 2000-fold excess over immunoconjugate at the highest antibody concentration) added. After incubation for 5 min at room temperature, the radiolabeling efficiency was assessed by ITLC as described above. The complete assay was carried out in triplicate and each ITLC was also run in triplicate.

### Serum stability assay

To 50 μg (25 μL) of each immunoconjugate was added $^{64}$Cu solution (12.5 MBq, 25 μL). Reactions were incubated at room temperature for 20 min (or at 37°C for 90 min in the case of DOTA-rituximab). The radioimmunoconjugates were added to 450 μL of male AB type human serum and incubated at 37°C for 48 h. Samples were analyzed by size exclusion HPLC at 0, 24 and 48 h using a BioSep SEC-S-2000 column (Phenomenex, Macclesfield, UK) with an isocratic mobile phase of 0.1 M phosphate buffer containing 2 mM EDTA, pH 7 and a flow rate of 1 mL/min. For the later time points when the signal from the HPLC in-line radionuclide detector was low, fractions from the HPLC were collected and counted in a gamma counter to measure the radioactivity. The amount of radioactivity associated with the antibody was assessed based on the retention time.

### Biodistribution study

Animal studies were carried out in accordance with UK Research Councils' and Medical Research Charities' guidelines on Responsibility in the Use of Animals in Bioscience Research, under a UK Home Office licence. Female BALB/c mice (n = 3 per group, aged 9 weeks, 20.6 ± 1.1 g) were purchased from Harlan Laboratories, UK. Each group received i.v. (tail vein) injections of approximately 6 MBq, 35 μL) of a $^{64}$Cu-labeled immunoconjugate. The feces and urine of each set of 3 mice were pooled due to logistic issues of housing the animals separately over 48 h. Animals were culled at 48 h post-injection and tissues explanted, weighed (except thyroid, *vide infra*) and counted on a gamma counter. The whole body activity (excluding tail) was measured with an ionization chamber cross-calibrated with the gamma counter, prior to dissection. Due to the small size and intimate attachment to trachea, normal thyroid glands were explanted along with a small piece of trachea and counted on the gamma counter. A small piece of trachea was also counted as a control. For all biodistribution calculations, a standard thyroid tissue mass of 0.0169 g (+/−0.0052) previously obtained from age-matched BALB/c mice (n = 14) was used. A separate piece of thyroid-free trachea was taken and weighed to confirm that activity in trachea tissue did not significantly affect the thyroid activity measurement. Uptake in each tissue was expressed as the percentage injected dose per gram of tissue (%ID/g). Excreted radioactivity, radioactivity in the tail, and mass of the tail were excluded from the calculation.

### Imaging study

BALB/c mouse (age and weight as above) received i.v. (tail vein) injections of 12 or 6 MBq of each radioimmunoconjugate (70 μL). With the mice under isofluorane anaesthesia in a Minerve imaging chamber, PET/CT scans were acquired 4 h, 24 h and 48 h post injection using a NanoPET/CT scanner (Bioscan, Paris, France) with PET acquisition time 1800 s,

1800 s and 3600 s respectively, coincidence relation: 1-3. Image reconstruction: OSEM with SSRB 2D LOR, energy window: 400-600 keV, filter: Ramlak cutoff 1, number of iterations/ subsets: 8/6. The biodistribution of the tracer in the imaged mice was then determined by dissection and organ counting after sacrificing at 48 h p.i.

## Results

### Conjugation and Radiolabeling

Immunoconjugates were prepared by conjugation of the BFCs through free amine groups on lysine residues within the antibody, either via a thiourea linkage (isothiocyanato derivatised chelators) or, in the case of sar-$CO_2H$, by amide formation (active *N*-hydroxysuccinimide ester-derived chelator). The average number of BFCs per antibody was 4.9 ± 0.9 (± SD, n = 4) for the isothiocyanato-derivatized chelators and 0.5 ± 0.1 (± SD, n = 4) for sar-$CO_2H$ (Table 1).

At a radioimmunoconjugate concentration of 13 μM, all immunoconjugates were labeled with $^{64}Cu^{2+}$ with high efficiency (see Figure 3 for example HPLC chromatograms). Size exclusion HPLC was able to resolve radiolabeled antibody from radiolabeled antibody aggregates and low molecular weight radiolabeled impurities. Radiochemical purity of all unpurified $^{64}$Cu-labeled immunoconjugates was 99.5% ± 0.5% except in the case of DTPA-rituximab where radiochemical purity was 96.8% ±1.8%. It is reported in the literature that DOTA-rituximab does not label well at room temperature[10, 65] so in this case the radiolabeling mixture was heated at 37°C but all other immunoconjugates were efficiently labeled at room temperature in 20 min.

However, further investigations into the radiolabeling of DOTA-rituximab under different conditions showed that, in our hands, there was no difference in the radiolabeling efficiency at the three temperatures studied (4-8°C, 25°C and 37°C). Labeling efficiency was 98.9% at all temperatures. There was also no difference in the amount of activity still associated with the immunoconjugate following challenge with EDTA (2000-fold molar excess), with 98.1 % still associated with DOTA-rituximab that had been labeled at 4-8°C and 98.2 % still associated with DOTA-rituximab that had been labeled at 25°C or 37°C.

To determine the relative efficacy of radiolabeling of the conjugates, increasingly dilute samples of the conjugates were studied. The most efficacious chelators were taken to be those that resulted in comparatively high radiochemical yields at lowest concentration of conjugate. Since the BFC-to-antibody ratio varied among the chelators, the concentrations were standardised on the effective BFC concentration rather than antibody concentration (by multiplying antibody concentration by the appropriate measured BFC-to-antibody-ratio). All immunoconjugates, with the exception of DTPA-rituximab (74.5%), labeled with >97% efficiency at an effective BFC concentration of 2500 nM (174 MBq/mg immunoconjugate). On reducing the immunoconjugate concentration to give an effective BFC concentration of 1250 nM, the radiolabeling efficiency after 20 min remained >90% for all immunconjugates, except DTPA-rituximab. At further reduced BFC concentrations, however, only NOTA-Rituximab, sar-CO-Rituximab, CHX-A”-DTPA-Rituximab and 2B3M-ITC-DTPA-Rituximab had labeling efficiency >90% (Figure 4). NOTA-Rituximab and sar-CO-

Rituximab achieved high radiolabeling efficiency under the most dilute conditions with 95.2 % (± 0.2%) and 97.7% (± 0.7%) labeling at approx. 120-150 nM effective BFC concentration (2775 MBq/mg or 416 MBq/nmol immunoconjugate in the case of NOTA-Rituximab).

### Serum Stability

Serum stability of all $^{64}$Cu-rituximab immunoconjugates was measured at 37°C over 48 h (Figure 5). A control using unconjugated rituximab subjected to the same labeling procedure as the conjugated rituximab showed minimal labeling (<2%) and "free" $^{64}$Cu eluted after the antibody peak on HPLC at approximately 11 min. $^{64}$Cu-rituximab immunoconjugates containing a macrocyclic BFC (*p*-SCN-Bn-DOTA, *p*-SCN-Bn-NOTA, *p*-SCN-Bn-oxo-DO3A, *p*-SCN-Bn-PCTA or sar-$CO_2$H) demonstrated greater radiochemical stability than immunoconjugates containing DTPA BFC derivatives. All macrocyclic conjugated immunoconjugates showed high stability in serum over 48 h with $^{64}$Cu-NOTA-rituximab showing the greatest stability (97.5% ± 0.3%) at 48 h. Stability of DTPA-based conjugates was much lower: 38.2% and 37.8% for $^{64}$Cu-CHX-A"-DTPA-rituximab and $^{64}$Cu-2B3M-DTPA-rituximab respectively. The most unstable radioimmunoconjugate was the unsubstituted $^{64}$Cu-DTPA-rituximab with only 14.0% of the radioactivity associated with the antibody at 48 h.

### Biodistribution and Imaging

Biodistribution and PET imaging studies were done on normal female Balb/c mice. Images were taken at 4, 24 and 48 h post-injection and biodistribution analyzed at 48 h. The results of the biodistribution (48 h) and imaging (24 h) studies are presented in Figures 6 and 7. For the immunoconjugates containing macrocycles, the activity was predominantly seen in the blood pool at all time points (4 h, 24 h and 48 h post-injection) with little difference seen in the biodistribution between the different macrocycles. Importantly, there is no difference between the macrocycle conjugates in the uptake in the kidneys and liver suggesting that all the macrocyclic radioimmunoconjugates show good stability *in vivo*. The clearance of the immunoconjugates containing DTPA derivatives from the blood pool was much faster compared with the immunoconjugates containing macrocycles, giving rise to higher liver to blood ratios and images dominated by liver and gut activity.

There was a higher level of excretion into the feces for the immunoconjugates containing DTPA derivatives (mean 29.8 %ID) compared to the macrocyclic immunoconjugates (mean 3.0 %ID) over 48 h. In addition, $^{64}$Cu-Oxo-DO3A-rituximab and $^{64}$Cu-PCTA-rituximab showed higher levels of excretion into the feces (3.7 % ID and 4.6% ID respectively) than $^{64}$Cu-DOTA-rituximab, $^{64}$Cu-NOTA-rituximab and $^{64}$Cu-sar-CO-rituximab over 48 h (2.2% ID, 2.9% ID and 1.6% ID, see Figure 8).

## Discussion

For the purposes of this study, rituximab was used as a model antibody to study the radiolabeling and stability of $^{64}$Cu-immunoconjugates. It is envisaged that the most

propitious conjugation and radiolabeling conditions elucidated here for rituximab can be translated to other antibodies, proteins and peptides.

Conjugation to each of the isothiocyanate-derivatised BFCs yielded approximately 5 chelators per antibody using identical conjugation conditions for each BFC. Where a different conjugation method was used (i.e. active ester, in the case of sar-$CO_2H$) the number of chelators per antibody was markedly reduced (0.5 chelator per antibody) but no attempt was made at this stage to optimize the conjugation to increase the number of chelators per antibody. It is possible that increasing the number of chelators bound to each antibody can lead to a decrease in immunoreactivity.

All of the rituximab immunoconjugates studied showed good radiolabeling efficiency at concentrations that are not kinetically or thermodynamically exacting (13 μM). Radiolabeling was carried out over 20 min at room temperature, except in the case of DOTA-rituximab. The slower radiolabeling for DOTA-metal ion complexes is well-documented[17]. Efficient radiolabeling of DOTA-peptides in short incubation periods is reported at high temperatures, but antibodies will not tolerate these conditions therefore radiolabeling of DOTA-immunoconjugates has usually been carried out at 40-43°C over a longer period of time [66-72], in order to achieve satisfactory labeling efficiency. In view of this, in this study, DOTA-rituximab radiolabeling was carried out at 37°C over 90 min.

To discriminate between the performance of the different BFC's under investigation the immunoconjugate concentration was reduced to determine radiolabeling efficiency under progressively more challenging conditions. It was found that whereas the labeling efficiency of several chelators (including the widely-used DOTA) dropped significantly when the chelator concentration dropped below 1μM, NOTA-rituximab and Sar-CO-rituximab could be radiolabeled efficiently under very dilute conditions (>90% radiolabeling efficiency at 125 nM chelator concentration in 20 min at room temperature when radiolabeled with 1.3 MBq $^{64}$Cu). This suggests that complex formation with NOTA and Sar-$CO_2H$ conjugates is faster than the other BFC's investigated in this study although it does not imply that they form the most kinetically or thermodynamically stable complexes. Even in the cases of NOTA-rituximab and Sar-CO-rituximab, where the specific activity achieved under these mild conditions is significantly higher than for the other chelators, the specific activities equate to roughly 1% of chelator molecules being occupied by a $^{64}$Cu ion. It is possible that yields and specific activities might be increased further by prolonging the incubation time or raising the temperature, and by introducing further steps to remove trace metals during the purification of $^{64}$Cu from the target material.

During the course of this work, it was observed that in our hands radiolabeling of DOTA-rituximab could be achieved in high yields (98.9 %) in 20 min at temperatures as low as 4-8°C, despite literature consensus that elevated temperatures are required for labeling DOTA-conjugated biomolecules with copper isotopes. Although neither we nor other groups working with $^{64}$Cu can provide analytical data to explain the contrasting experience, we note that in the work described here we used fraction 9 from the ion exchange purification of $^{64}$Cu, rather than fraction 8 which contains the most $^{64}$Cu, because fraction 9 consistently gave better labeling yields and less antibody aggregation and precipitation. Fraction 8 is

more acidic before buffering (as determined with a pH elecetrode), has higher chloride concentration, and may have a different trace metal content, than fraction 9; one or more of these factors may contribute to the less efficient labeling using this fraction. Further investigation is required to identify the cause of inefficient labeling with fraction 8 and to improve the purification procedure accordingly, since fraction 8 contains the majority of the $^{64}$Cu radioactivity.

The stability of the radioimmunoconjugates was assessed in serum and *in vivo*. In the control, there was no evidence of $^{64}$Cu transchelation to serum proteins that was not in turn transchelated to EDTA during the HPLC analysis, therefore it is reasonable to assume that radioactivity eluting in the high molecular weight fraction is antibody-bound. All the macrocyclic chelated immunoconjugates were very stable in serum but the immunoconjugates containing DTPA derivatives were unstable with released copper which appeared at an elution time corresponding to the copper EDTA complex. Ferreira *et al.*[72] observed a difference in the stability of three $^{64}$Cu-trastuzumab radioimmunoconjugates: the immunoconjugates $^{64}$Cu-PCTA-trastuzumab and $^{64}$Cu-Oxo-DO3A-trastuzumab (>95% intact at 24 h and ~80% intact at 48 h) were more stable in serum than $^{64}$Cu-DOTA-trastuzumab (54% intact at 24 h and 26% intact at 48 h). In contrast, we found little difference between the macrocyclic immunoconjugates with all showing high labeling efficiency and >95% stability at 24 h and >94.9% at 48 h. The labeled conjugates could be used without additional purification. We speculate that the comparatively high labeling efficiency and stability we find compared to others [21, 72, 73] may be related to our use of fraction 9 from the $^{64}$Cu purification.

It is interesting to note that while the efficiency of labeling for $^{64}$Cu-2B3M-DTPA-rituximab and $^{64}$Cu-CHX-A”-DTPA-rituximab is favorable, the resulting radiolabeled immunoconjugates do not demonstrate adequate serum stability. In contrast, $^{64}$Cu-NOTA-rituximab and $^{64}$Cu-sar-CO-rituximab were both found to offer both favorable rapid labeling and very high complex stability in serum. In the biodistribution study, $^{64}$Cu-DTPA-, $^{64}$Cu-2B3M-DTPA- and $^{64}$Cu-CHX-A”-DTPA-rituximab, which all showed poor serum stability, were rapidly cleared from the blood pool and the activity was predominantly excreted into the feces (approximately 30% of the injected dose) by 48 h. In contrast, the macrocycle-containing immunoconjugates showed predominantly blood pool activity and there was no difference in the biodistribution of these immunoconjugates at 48 h. Most notably, there was no difference in the liver and kidney uptake among the radioimmunoconjugates. It has been reported that $^{64}$Cu-DOTA conjugates can lose $^{64}$Cu to proteins such as superoxide dismutase, possibly via bioreductive mechanisms, with the $^{64}$Cu being retained in the liver[44]. There was no evidence of a higher liver retention of $^{64}$Cu in these studies. It was noted, however, that there was slightly higher activity in the feces of animals injected with $^{64}$Cu-Oxo-DO3A-rituximab and $^{64}$Cu-PCTA-rituximab over the course of the study. Ferreira *et al.*[72] showed similar biodistribution results for $^{64}$Cu-DOTA-trastuzumab, $^{64}$Cu-Oxo-DO3A-trastuzumab and $^{64}$Cu-PCTA-trastuzumab but noted higher uptake in the tumors of tumor-bearing animals for $^{64}$Cu-Oxo-DO3A-trastuzumab and $^{64}$Cu-PCTA-trastuzumab.

The biodistribution of $^{64}$Cu-complex conjugates has previously been shown to be influenced by the charge and lipophilicity of the complexes[23, 35] but these studies were carried out on antibody fragments rather than intact antibodies. The smaller size of these fragments will make their biodistribution more susceptible to the influence of the nature of the BFC, compared to intact antibodies. For intact antibodies, the performance of the BFC itself in terms of the stability of the $^{64}$Cu-complex, the stability of the chelate-antibody conjugate, the radiolabeling efficiency and convenience of radiolabeling are much more important factors. From the *in vivo* study presented here, where the different immunoconjugates were labeled to the same specific activity and achieved the same radiolabeling efficiency, we found little difference in the stability of the complexes and the physical characteristics of the chelators did not influence the biodistribution.

Quadri and Vriesendorf[74] demonstrated that the linker could be crucial determinant of biodistribution. Labile linkers can be cleaved from the antibody by enzymes in the serum and liver giving rise to low molecular weight radioactive metabolites which will tend to be cleared via the kidneys. Isothiocyanatobenzyl (*p*-SCN-Bn) derivatives form a stable thiourea bond with the amino side chain of lysine residues and are therefore a good choice of linker for connecting the chelator to the antibody. However, we found no difference in the *in vivo* stability of the thiourea conjugated immunoconjugates and the amide conjugated sar-CO-rituximab.

It is intuitively clear that thermodynamic stability alone (as expressed, for example, by low metal-ligand dissociation constants) is not a sound basis on which to select a chelator to make immunoconjugates with the best *in vivo* stability, since under biological conditions at tracer levels, if allowed to come to equilibrium, even complexes with very high stability constants (such as the NOTA and DTPA complexes of copper) would not withstand challenge from endogenous metal-binding proteins, endogenous metal ions, metabolism and extreme dilution. Our results show no correlation between $Cu^{2+}$ complex stability constants and serum stability. Indeed, reported stability constants for $Cu^{2+}$ complexes of NOTA and DTPA are comparable (log*K* values of 21.6 and 21.4 respectively[5]) yet the serum stability of the $^{64}$Cu-labeled conjugates is markedly different (97.5 ± 3.0% vs 14.0 ± 12.9% antibody-bound $^{64}$Cu after 48 h respectively). Dearling *et al*.[21] also recently showed that differences in the thermodynamic stability of $^{64}$Cu-BFC complexes were not associated with significant differences in uptake of radioimmunoconjugates by tumors; indeed, the least thermodynamically stable copper complex that they studied, $^{64}$Cu-NOTA, produced the lowest concentration of $^{64}$Cu in the liver. Similarly, Cole *et al*.[18] found that thermodynamic equilibrium constants of $^{67}$Cu-, $^{111}$In- and $^{57}$Co-radiometal complexes bore little relation to the serum stability of the complexes. In particular, the published thermodynamic equilibrium constants suggest that $^{67}$Cu-TETA would be less stable than $^{67}$Cu-DTPA or $^{67}$Cu-EDTA whereas $^{67}$Cu-TETA was the only complex of the three to show any stability in serum. Such macrocyclic or macrobicyclic $Cu^{2+}$ complexes possess sufficiently high thermodynamic stability to allow efficient radiolabeling, as well as relatively rigid geometries that enhance their kinetic stability[8, 10, 75, 76]. Individual bond dissociation is rapidly followed by re-coordination, as the coordinating ligand remains spatially close to the metal centre. A sufficiently low reduction potential of the bound $Cu^{2+}$ metal centre is also desirable, as

intracellular endogenous reductants, such as thiol-rich proteins, are capable of reducing $Cu^{2+}$ to $Cu^{+}$[75, 77]. $Cu^{+}$, with a $d^{10}$ configuration, possesses markedly different coordination preferences to $Cu^{2+}$ and is more kinetically labile, and can dissociate from the chelate in the presence of in vivo endogenous cuprous-binding ligands.

To achieve the required *in vivo* stability requires that equilibration is delayed as long as possible, maximizing kinetic stability by imposing high activation free energy barriers to dissociation. However, these same free-energy barriers have to be overcome in order to perform the radiolabeling, therefore the optimal chelator design will require balancing both efficiency of labeling (requiring a low free energy barrier between complexed and dissociated states) and resistance to dissociation *in vivo* (requiring a high free energy barrier). Identifying chelators with the appropriate compromise is at present largely an empirical matter, and side-by-side comparison of chelators in the context of a bioconjugate is necessary. Assessing the *in vivo* stability and biodistribution combined with the stability in serum and the ability of the ligand to complex radiometal under increasingly dilute conditions, as described here, provides a discriminating and systematic approach for assessing which BFC is appropriate for any given radiometal.

## Conclusion

The results presented here suggest that *p*-SCN-NOTA and sar-$CO_2H$ stand out from the other chelators, including the commonly used DOTA, as the most promising BFCs for radiolabeling antibodies with $^{64}Cu$. Dearling *et al.*[21] report good efficacy for *p*-SCN-NOTA and Liu *et al.*[78] found that employing the NOTA chelator in studies using $^{64}Cu$-labeled heat-stable enterotoxin analogues for detecting colorectal cancer gave superior tumor/liver and tumor/kidney ratios relative to DOTA- and TETA-functionalized peptides. The prolonged retention in blood pool and the low amount of activity in the feces and urine in our study suggest that $^{64}Cu$-NOTA-rituximab and $^{64}Cu$-sar-CO-rituximab are extremely stable *in vivo*, while labeling is rapid and easy under mild conditions and achieves high specific activity under very dilute conditions. These properties make them very attractive as $^{64}Cu$-complexing BFCs for radiolabeling antibodies.

## Supplementary Material

Refer to Web version on PubMed Central for supplementary material.

## Acknowledgements

MSC, KPS and JDW were supported by the King's College London-UCL Comprehensive Cancer Imaging Centre funded by Cancer Research UK & EPSRC, in association with MRC and DoH (UK). MTM acknowledges: Cancer Council Victoria for providing a Sydney Parker Smith Postdoctoral Cancer Research Fellowship; The State Government of Victoria for a Victoria Fellowship; and a Kaye Merlin Brutton Bequest. PSD acknowledges financial support from the Australian Research Council. We thank Wellcome Trust for grant support to PJB enabling purchase of the PET-CT scanner. RP was supported in part by a National Institute for Health Research (NIHR) comprehensive Biomedical Research Centre award to Guy's & St Thomas' NHS Foundation Trust in partnership with King's College London and King's College Hospital NHS Foundation Trust, and in part by the Guy's and St Thomas' Charity. We thank Stephen Clarke (supported by the Centre of Excellence in Medical Engineering funded by the Wellcome Trust and EPSRC under grant WT 088641/Z/09/Z) for assistance with PET/CT imaging. We thank Levente Meszeros (supported by a Cancer Research UK studentship), Alex Koers

(supported by a National Institute for Health Research-funded Biomedical Research Centre studentship) and Alex O'Neill (supported by the Harris studentship) for assistance with biodistribution studies.

## References

(1). Meares CF, Goodwin DA. Linking radiometals to proteins with bifuntional chelating agents. J. Protein Chem. 1984; 3:215–28.

(2). Blower PJ, Lewis JS, Zweit J. Copper radionuclides and radiopharmaceuticals in nuclear medicine. Nucl. Med. Biol. 1996; 23:957–80. [PubMed: 9004284]

(3). Donnelly PS. The role of coordination chemistry in the development of copper and rhenium radiopharmaceuticals. Dalton Trans. 2011; 40:999–1010. [PubMed: 21203624]

(4). Zamora PO, Mercer-Smith JA, Marek MJ, Schulte LD, Rhodes BA. Similarity of copper and technetium binding sites in human IgG. Nucl. Med. Biol. 1992; 19:797–802.

(5). Wadas TJ, Wong EH, Weisman GR, Anderson CJ. Coordinating radiometals of copper, gallium, indium, yttrium, and zirconium for PET and SPECT imaging of disease. Chem. Rev. 2010; 110:2858–902. [PubMed: 20415480]

(6). Motekaitis RJ, Rogers BE, Reichert DE, Martell AE, Welch MJ. Stability and structure of activated macrocycles. Ligands with biological applications. Inorg. Chem. 1996; 35:3821–7. [PubMed: 11666570]

(7). Sun X, Wuest M, Weisman GR, Wong EH, Reed DP, Boswell CA, Motekaitis R, Martell AE, Welch MJ, Anderson CJ. Radiolabeling and in vivo behavior of copper-64-labeled cross-bridged cyclam ligands. J. Med. Chem. 2002; 45:469–77. [PubMed: 11784151]

(8). Ma MT, Donnelly PS. Peptide targeted copper-64 radiopharmaceuticals. Curr. Top. Med. Chem. 2011; 11:500–20. [PubMed: 21189129]

(9). Wong EH, Weisman GR, Hill DC, Reed DP, Rogers ME, Condon JS, Fagan MA, Calabrese JC, Lam K-C, Guzei IA, Rheingold AL. Synthesis and characterization of cross-bridged cyclams and pendant-armed derivatives and structural studies of their copper(II) complexes. J. Am. Chem. Soc. 2000; 122:10561–72.

(10). Smith SV. Molecular imaging with copper-64. J. Inorg. Biochem. 2004; 98:1874–901. [PubMed: 15522415]

(11). McMurry TJ, Brechbiel M, Wu C, Gansow OA. Synthesis of 2-(*p*-thiocyanatobenzyl)-1,4,7-triazacyclononane-1,4,7-triacetic acid: Application of the 4-methoxy-2,3,6-trimethylbenzenesulfonamide protecting group in the synthesis of macrocyclic polyamines. Bioconjugate Chem. 1993; 4:236–45.

(12). Anderson CJ, Welch MJ. Radiometal-labeled agents (non-technetium) for diagnostic imaging. Chem. Rev. 1999; 99:2219–34. [PubMed: 11749480]

(13). Eisenwiener KP, Powell P, Macke HR. A convenient synthesis of novel bifunctional prochelators for coupling to bioactive peptides for radiometal labelling. Bioorg. Med. Chem. Lett. 2000; 10:2133–5. [PubMed: 10999487]

(14). Gasser G, Tjioe L, Graham B, Belousoff MJ, Juran S, Walther M, Kuenstler J-U, Bergmann R, Stephan H, Spiccia L. Synthesis, copper(II) complexation, $^{64}$Cu-labeling, and bioconjugation of a new bis(2-pyridylmethyl) derivative of 1,4,7-triazacyclononane. Bioconjugate Chem. 2008; 19:719–30.

(15). Juran S, Walther M, Stephan H, Bergmann R, Steinbach J, Kraus W, Emmerling F, Comba P. Hexadentate bispidine derivatives as versatile bifunctional chelate agents for copper(II) radioisotopes. Bioconjugate Chem. 2009; 20:347–59.

(16). Roehrich A, Bergmann R, Kretzschmann A, Noll S, Steinbach J, Pietzsch J, Stephan H. A novel tetrabranched neurotensin(8-13) cyclam derivative: Synthesis, $^{64}$Cu-labeling and biological evaluation. J. Inorg. Biochem. 2011; 105:821–32. [PubMed: 21497581]

(17). Brechbiel MW. Bifunctional chelates for metal nuclides. Q. J. Nucl. Med. Mol. Imaging. 2008; 52:166–73. [PubMed: 18043537]

(18). Cole WC, DeNardo SJ, Meares CF, McCall MJ, DeNardo GL, Epstein AL, O'Brien HA, Moi MK. Serum stability of $^{67}$Cu chelates: comparison with $^{111}$In and $^{57}$Co. Int. J. Rad. Appl. Instrum. B. 1986; 13:363–8. [PubMed: 3539884]

(19). Kukis DL, Diril H, Greiner DP, DeNardo SJ, DeNardo GL, Salako QA, Meares CF. A comparative study of copper-67 radiolabeling and kinetic stabilities of antibody-macrocycle chelate conjugates. Cancer. 1994; 73:779–86. [PubMed: 8306260]

(20). Lewis MR, Boswell CA, Laforest R, Buettner TL, Ye D, Connett JM, Anderson CJ. Conjugation of monoclonal antibodies with TETA using activated esters: Biological comparison of $^{64}$Cu-TETA-1A3 with $^{64}$Cu-BAT-2IT-1A3. Cancer Biother. Radiopharm. 2001; 16:483–94. [PubMed: 11789025]

(21). Dearling JLJ, Voss SD, Dunning P, Snay E, Fahey F, Smith SV, Huston JS, Meares CF, Treves ST, Packard AB. Imaging cancer using PET - the effect of the bifunctional chelator on the biodistribution of a $^{64}$Cu-labeled antibody. Nucl. Med. Biol. 2011; 38:29–38. [PubMed: 21220127]

(22). Zimmermann K, Grunberg J, Honer M, Ametamey S, Schubiger PA, Novak-Hofer I. Targeting of renal carcinoma with $^{67/64}$Cu-labeled anti-L1-CAM antibody chCE7: selection of copper ligands and PET imaging. Nucl. Med. Biol. 2003; 30:417–27. [PubMed: 12767399]

(23). Rogers BE, Anderson CJ, Connett JM, Guo LW, Edwards WB, Sherman ELC, Zinn KR, Welch MJ. Comparison of four bifunctional chelates for radiolabeling monoclonal antibodies with copper radioisotopes: Biodistribution and metabolism. Bioconjugate Chem. 1996; 7:511–22.

(24). Roselli M, Schlom J, Gansow OA, Brechbiel MW, Mirzadeh S, Pippin CG, Milenic DE, Colcher D. Comparative biodistribution studies of DTPA-derivative bifunctional chelates for radiometal labeled monoclonal antibodies. Int. J. Rad. Appl. Instrum. B. 1991; 18:389–94. [PubMed: 1864727]

(25). Novak-Hofer I, Amstutz HP, Maecke HR, Schwarzbach R, Zimmermann K, Morgenthaler J-J, Schubiger PA. Cellular processing of copper-67-labeled monoclonal antibody chCE7 by human neuroblastoma cells. Cancer Res. 1995; 55:46–50. [PubMed: 7805039]

(26). Smith A, Alberto R, Blaeuenstein P, Novak-Hofer I, Maecke HR, Schubiger PA. Preclinical evaluation of copper-67-labeled intact and fragmented anti-colon carcinoma monoclonal antibody MAb35. Cancer Res. 1993; 53:5727–33. [PubMed: 8242629]

(27). Smith-Jones PM, Fridrich R, Kaden TA, Novak-Hofer I, Siebold K, Tschudin D, Maecke HR. Antibody labeling with copper-67 using the bifunctional macrocycle 4-[(1,4,8,11-tetraazacyclotetradec-1-yl)methyl]benzoic acid. Bioconjugate Chem. 1991; 2:415–21.

(28). Anderson CJ, Connett JM, Schwarz SW, Rocque PA, Guo LW, Philpott GW, Zinn KR, Meares CF, Welch MJ. Copper-64-labeled antibodies for PET imaging. J. Nucl. Med. 1992; 33:1685–90. [PubMed: 1517844]

(29). Anderson CJ, Schwarz SW, Connett JM, Cutler PD, Guo LW, Germain CJ, Philpott GW, Zinn KR, Greiner DP, Meares CF, Welch MJ. Preparation, biodistribution and dosimetry of copper-64-labeled anti-colorectal carcinoma monoclonal antibody fragments 1A3-F(ab')$_2$. J. Nucl. Med. 1995; 36:850–8. [PubMed: 7738663]

(30). Connett JM, Anderson CJ, Guo L-W, Schwarz SW, Zinn KR, Rogers BE, Siegel BA, Philpott G, Welch MJ. Radioimmunotherapy with a $^{64}$Cu-labeled monoclonal antibody: a comparison with $^{67}$Cu. Proc. Natl. Acad. Sci. U. S. A. 1996; 93:6814–8. [PubMed: 8692901]

(31). Franz J, Freeman GM, Barefield EK, Volkert WA, Ehrhardt GJ, Holmes RA. Labeling of antibodies with copper-64 using a conjugate containing a macrocyclic amine chelating agent. Nucl. Med. Biol. 1987; 14:479–84.

(32). Lewis MR, Wang M, Axworthy DB, Theodore LJ, Mallet RW, Fritzberg AR, Welch MJ, Anderson CJ. In vivo evaluation of pretargeted $^{64}$Cu for tumor imaging and therapy. J. Nucl. Med. 2003; 44:1284–92. [PubMed: 12902420]

(33). Morphy JR, Parker D, Alexander R, Bains A, Carne AF, Eaton MAW, Harrison A, Millican A, Phipps A, Rhind SK, Titmas R, Weatherby D. Antibody labeling with functionalized cyclam macrocycles. J. Chem. Soc., Chem. Commun. 1988:156–8.

(34). Wu AM, Yazaki PJ, Tsai S-W, Nguyen K, Anderson A-L, McCarthy DW, Welch MJ, Shively JE, Williams LE, Raubitschek AA, Wong JYC, Toyokuni T, Phelps ME, Gambhir SS. High-resolution microPET imaging of carcinoembryonic antigen-positive xenografts by using a copper-64-labeled engineered antibody fragment. Proc. Natl. Acad. Sci. U. S. A. 2000; 97:8495–500. [PubMed: 10880576]

(35). Jones-Wilson TM, Deal KA, Anderson CJ, McCarthy DW, Kovacs Z, Motekaitis RJ, Sherry AD, Martell AE, Welch MJ. The in vivo behavior of copper-64-labeled azamacrocyclic complexes. Nucl. Med. Biol. 1998; 25:523–30. [PubMed: 9751418]

(36). Prasanphanich AF, Nanda PK, Rold TL, Ma L, Lewis MR, Garrison JC, Hoffman TJ, Sieckman GL, Figueroa SD, Smith CJ. [$^{64}$Cu-NOTA-8-Aoc-BBN(7-14)$NH_2$] targeting vector for positron-emission tomography imaging of gastrin-releasing peptide receptor-expressing tissues. Proc. Natl. Acad. Sci. U. S. A. 2007; 104:12462–7. [PubMed: 17626788]

(37). Boswell CA, Sun X, Niu W, Weisman GR, Wong EH, Rheingold AL, Anderson CJ. Comparative in vivo stability of copper-64-labeled cross-bridged and conventional tetraazamacrocyclic complexes. J. Med. Chem. 2004; 47:1465–74. [PubMed: 14998334]

(38). Fani M, Del Pozzo L, Abiraj K, Mansi R, Tamma ML, Cescato R, Waser B, Weber WA, Reubi JC, Maecke HR. PET of somatostatin receptor-positive tumors using $^{64}$Cu- and $^{68}$Ga-somatostatin antagonists: the chelate makes the difference. J. Nucl. Med. 2011; 52:1110–8. [PubMed: 21680701]

(39). Lewis JS, Lewis MR, Srinivasan A, Schmidt MA, Wang J, Anderson CJ. Comparison of four $^{64}$Cu-labeled somatostatin analogs in vitro and in a tumor-bearing rat model: Evaluation of new derivatives for positron emission tomography imaging and targeted radiotherapy. J. Med. Chem. 1999; 42:1341–7. [PubMed: 10212119]

(40). Hausner SH, Kukis DL, Gagnon MKJ, Stanecki CE, Ferdani R, Marshall JF, Anderson CJ, Sutcliffe JL. Evaluation of [$^{64}$Cu]Cu-DOTA and [$^{64}$Cu]Cu-CB-TE2A chelates for targeted positron emission tomography with an αvβ6-specific peptide. Mol. Imaging. 2009; 8:111–21. [PubMed: 19397856]

(41). Heroux KJ, Woodin KS, Tranchemontagne DJ, Widger PCB, Southwick E, Wong EH, Weisman GR, Tomellini SA, Wadas TJ, Anderson CJ, Kassel S, Golen JA, Rheingold AL. The long and short of it: The influence of *N*-carboxyethyl versus *N*-carboxymethyl pendant arms on in vitro and in vivo behavior of copper complexes of cross-bridged tetraamine macrocycles. Dalton Trans. 2007:2150–62. [PubMed: 17514336]

(42). Meares CF, Moi MK, Diril H, Kukis DL, McCall MJ, Deshpande SV, DeNardo SJ, Snook D, Epenetos AA. Macrocyclic chelates of radiometals for diagnosis and therapy. Br. J. Cancer. 1990; 62(Suppl. X):21–6.

(43). Mirick GR, O'Donnell RT, DeNardo SJ, Shen S, Meares CF, DeNardo GL. Transfer of copper from a chelated $^{67}$Cu-antibody conjugate to ceruloplasmin in lymphoma patients. Nucl. Med. Biol. 1999; 26:841–5. [PubMed: 10628566]

(44). Bass LA, Wang M, Welch MJ, Anderson CJ. In vivo transchelation of copper-64 from TETA-octreotide to superoxide dismutase in rat liver. Bioconjugate Chem. 2000; 11:527–32.

(45). Ma MT, Cooper MS, Paul RL, Shaw KP, Karas JA, Scanlon D, White JM, Blower PJ, Donnelly PS. Macrobicyclic cage amine ligands for copper radiopharmaceuticals: A single bivalent cage amine containing two Lys$^3$-bombesin targeting peptides. Inorg. Chem. 2011; 50:6701–10. [PubMed: 21667932]

(46). Ma MT, Karas JA, White JM, Scanlon D, Donnelly PS. A new bifunctional chelator for copper radiopharmaceuticals: A cage amine ligand with a carboxylate functional group for conjugation to peptides. Chem. Commun. 2009:3237–9.

(47). Sargeson AM. Encapsulated metal ions. Pure Appl. Chem. 1984; 56:1603–19.

(48). Geue RJ, Hambley TW, Harrowfield JM, Sargeson AM, Snow MR. Metal ion encapsulation: Cobalt cages derived from polyamines, formaldehyde, and nitromethane. J. Am. Chem. Soc. 1984; 106:5478–88.

(49). Sargeson AM. The potential for the cage complexes in biology. Coord. Chem. Rev. 1996; 151:89–114.

(50). Sargeson AM. Developments in the synthesis and reactivity of encapsulated metal ions. Pure Appl. Chem. 1986; 58:1511–22.

(51). Bottomley GA, Clark IJ, Creaser II, Engelhardt LM, Geue RJ, Hagen KS, Harrowfield JM, Lawrance GA, Lay PA, Sargeson AM, See AJ, Skelton BW, White AH, Wilner FR. The synthesis and structure of encapsulating ligands: Properties of bicyclic hexamines. Aust. J. Chem. 1994; 47:143–79.

(52). Bernhardt PV, Harrowfield JM, Hockless DCR, Sargeson AM. *N*-Methylated macrobicyclic hexaamines of copper(II) and nickel(II): Large steric effects. Inorg. Chem. 1994; 33:5659–70.

(53). Di Bartolo NM, Sargeson AM, Donlevy TM, Smith SV. Synthesis of a new cage ligand, SarAr, and its complexation with selected transition metal ions for potential use in radioimaging. J. Chem. Soc., Dalton Trans. 2001:2303–9.

(54). Donnelly PS, Harrowfield JM. Synthesis with coordinated ligands: Biomolecule attachment to cage amines. J. Chem. Soc., Dalton Trans. 2002:906–13.

(55). Donnelly PS, Harrowfield JM, Skelton BW, White AH. Carboxymethylation of cage amines: Control of alkylation by metal ion coordination. Inorg. Chem. 2000; 39:5817–30. [PubMed: 11151385]

(56). Donnelly PS, Harrowfield JM, Skelton BW, White AH. Carboxymethylated cage amines: Coordination and lactamization. Inorg. Chem. 2001; 40:5645–52. [PubMed: 11599965]

(57). Di Bartolo N, Sargeson AM, Smith SV. New 64Cu PET imaging agents for personalised medicine and drug development using the hexa-aza cage. Org. Biomol. Chem. 2006; 4:3350–7. [PubMed: 17036125]

(58). Voss SD, Smith SV, DiBartolo N, McIntosh LJ, Cyr EM, Bonab AA, Dearling JLJ, Carter EA, Fischman AJ, Treves ST, Gillies SD, Sargeson AM, Huston JS, Packard AB. Positron emission tomography (PET) imaging of neuroblastoma and melanoma with $^{64}$Cu-SarAr immunoconjugates. Proc. Natl. Acad. Sci. U. S. A. 2007:1–5.

(59). Ma MT, Neels OC, Denoyer D, Roselt P, Karas JA, Scanlon DB, White JM, Hicks RJ, Donnelly PS. Gallium-68 complex of a macrobicyclic cage amine chelator tethered to two integrin-targeting peptides for diagnostic tumor imaging. Bioconjugate Chem. 2011; 22:2093–103.

(60). Lears KA, Ferdani R, Liang K, Zheleznyak A, Andrews R, Sherman CD, Achilefu S, Anderson CJ, Rogers BE. In vitro and in vivo evaluation of $^{64}$Cu-labeled SarAr-bombesin analogs in gastrin-releasing peptide receptor-expressing prostate cancer. J. Nucl. Med. 2011; 52:470–7. [PubMed: 21321264]

(61). Cai H, Li Z, Huang C-W, Shahinian AH, Wang H, Park R, Conti PS. Evaluation of copper-64 labeled AmBaSar conjugated cyclic RGD peptide for improved microPET imaging of integrin αvβ3 expression. Bioconjugate Chem. 2010; 21:1417–24.

(62). Cooper MS, Sabbah E, Mather SJ. Conjugation of chelating agents to proteins and radiolabeling with trivalent metallic isotopes. Nat. Protoc. 2006; 1:314–7. [PubMed: 17406251]

(63). Meares CF, McCall MJ, Reardan DT, Goodwin DA, Diamanti CI, McTigue M. Conjugation of antibodies with bifunctional chelating agents: isothiocyanate and bromoacetamide reagents, methods of analysis, and subsequent addition of metal ions. Anal. Biochem. 1984; 142:68–78. [PubMed: 6440451]

(64). Langford JH, Cooper MS, Orchard KH. Development and validation of the $^{57}$Co assay for determining the ligand to antibody ratio in bifunctional chelate/antibody conjugates for use in radioimmunotherapy. Nucl. Med. Biol. 2011; 38:1103–10. [PubMed: 21741259]

(65). Huang C-W, Li Z, Cai H, Shahinian T, Conti Peter S. Biological stability evaluation of the α2β1 receptor imaging agents: Diamsar and DOTA conjugated DGEA peptide. Bioconjugate Chem. 2011; 22:256–63.

(66). Li WP, Meyer LA, Capretto DA, Sherman CD, Anderson CJ. Receptor-Binding, Biodistribution, and Metabolism Studies of $^{64}$Cu-DOTA-Cetuximab, a PET-Imaging Agent for Epidermal Growth-Factor Receptor-Positive Tumors. Cancer Biother. Radiopharm. 2008; 23:158–71. [PubMed: 18454685]

(67). Cai W, Chen K, He L, Cao Q, Koong A, Chen X. Quantitative PET of EGFR expression in xenograft-bearing mice using $^{64}$Cu-labeled cetuximab, a chimeric anti-EGFR monoclonal antibody. Eur. J. Nucl. Med. Mol. Imaging. 2007; 34:850–8. [PubMed: 17262214]

(68). Lewis MR, Kao JY, Anderson A-LJ, Shively JE, Raubitschek A. An improved method for conjugating monoclonal antibodies with *N*-hydroxysulfosuccinimidyl DOTA. Bioconjugate Chem. 2001; 12:320–4.

(69). Cai W, Wu Y, Chen K, Cao Q, Tice David A, Chen X. In vitro and in vivo characterization of $^{64}$Cu-labeled Abegrin, a humanized monoclonal antibody against integrin αvβ3. Cancer Res. 2006; 66:9673–81. [PubMed: 17018625]

(70). Paudyal P, Paudyal B, Hanaoka H, Oriuchi N, Iida Y, Yoshioka H, Tominaga H, Watanabe S, Watanabe S, Ishioka NS, Endo K. Imaging and biodistribution of Her2/neu expression in non-small cell lung cancer xenografts with $^{64}$Cu-labeled trastuzumab PET. Cancer Science. 2010; 101:1045–50. [PubMed: 20219072]

(71). Martin SM, O'Donnell RT, Kukis DL, Abbey CK, McKnight H, Sutcliffe JL, Tuscano JM. Imaging and pharmacokinetics of $^{64}$Cu-DOTA-HB22.7 administered by intravenous, intraperitoneal, or subcutaneous injection to mice bearing non-Hodgkin's lymphoma xenografts. Mol. Imaging Biol. 2009; 11:79–87. [PubMed: 18949521]

(72). Ferreira C, L. Yapp D, T. T. Crisp S, Sutherland B, W. Ng Sylvia SW, Gleave M, Bensimon C, Jurek P, Kiefer G, E. Comparison of bifunctional chelates for (64)Cu antibody imaging. Eur. J. Nucl. Med. Mol. Imaging. 2010; 37:2117–26. [PubMed: 20552190]

(73). Ferreira CL, Yapp DT, Lamsa E, Gleave M, Bensimon C, Jurek P, Kiefer GE. Evaluation of novel bifunctional chelates for the development of Cu-64-based radiopharmaceuticals. Nucl. Med. Biol. 2008; 35:875–82. [PubMed: 19026949]

(74). Quadri SM, Vriesendorp HM. Effects of linker chemistry on the pharmacokinetics of radioimmunoconjugates. Q. J. Nucl. Med. 1998; 42:250–61. [PubMed: 9973840]

(75). Woodin KS, Heroux KJ, Boswell CA, Wong EH, Weisman GR, Niu W, Tomellini SA, Anderson CJ, Zakharov LN, Rheingold AL. Kinetic inertness and electrochemical behavior of copper(II) tetraazamacrocyclic complexes: Possible implications for in vivo stability. Eur. J. Inorg. Chem. 2005:4829–33.

(76). Shokeen M, Anderson CJ. Molecular imaging of cancer with copper-64 radiopharmaceuticals and positron emission tomography (PET). Acc. Chem. Res. 2009; 42:832–41. [PubMed: 19530674]

(77). Xiao Z, Donnelly PS, Zimmermann M, Wedd AG. Transfer of copper between bis(thiosemicarbozone ligands and intracellcular copper-binding proteins. Insights in mechanisms of copper uptake and selectivity. Inorg. Chem. 2008; 47:4338–47. [PubMed: 18412332]

(78). Liu D, Overbey D, Watkinson LD, Smith CJ, Daibes-Figueroa S, Hoffman TJ, Forte LR, Volkert WA, Giblin MF. Comparative evaluation of three 64Cu-labeled E. Coli heat-stable enterotoxin analogues for PET imaging of colorectal cancer. Bioconjugate Chem. 2010; 21:1171–6.

Europe PMC Funders Author Manuscripts

Europe PMC Funders Author Manuscripts

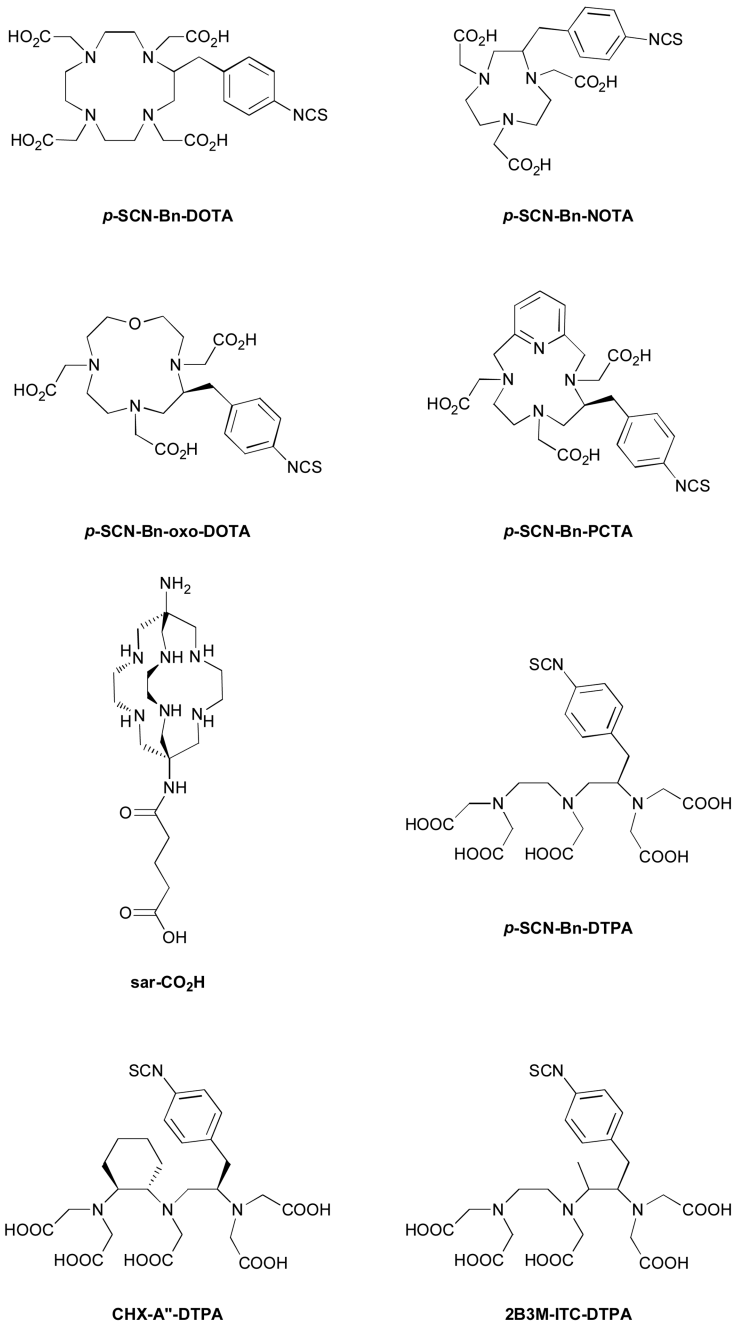


**Figure 1.**

Structures of bifunctional chelators *p*-SCN-Bn-DOTA, *p*-SCN-Bn-NOTA, *p*-SCNBn-oxo-DO3A, *p*-SCN-Bn-PCTA, sar-$CO_2$H, *p*-SCN-Bn-DTPA, CHX-A”-DTPA, 2B3M-ITC-DTPA.

Europe PMC Funders Author Manuscripts

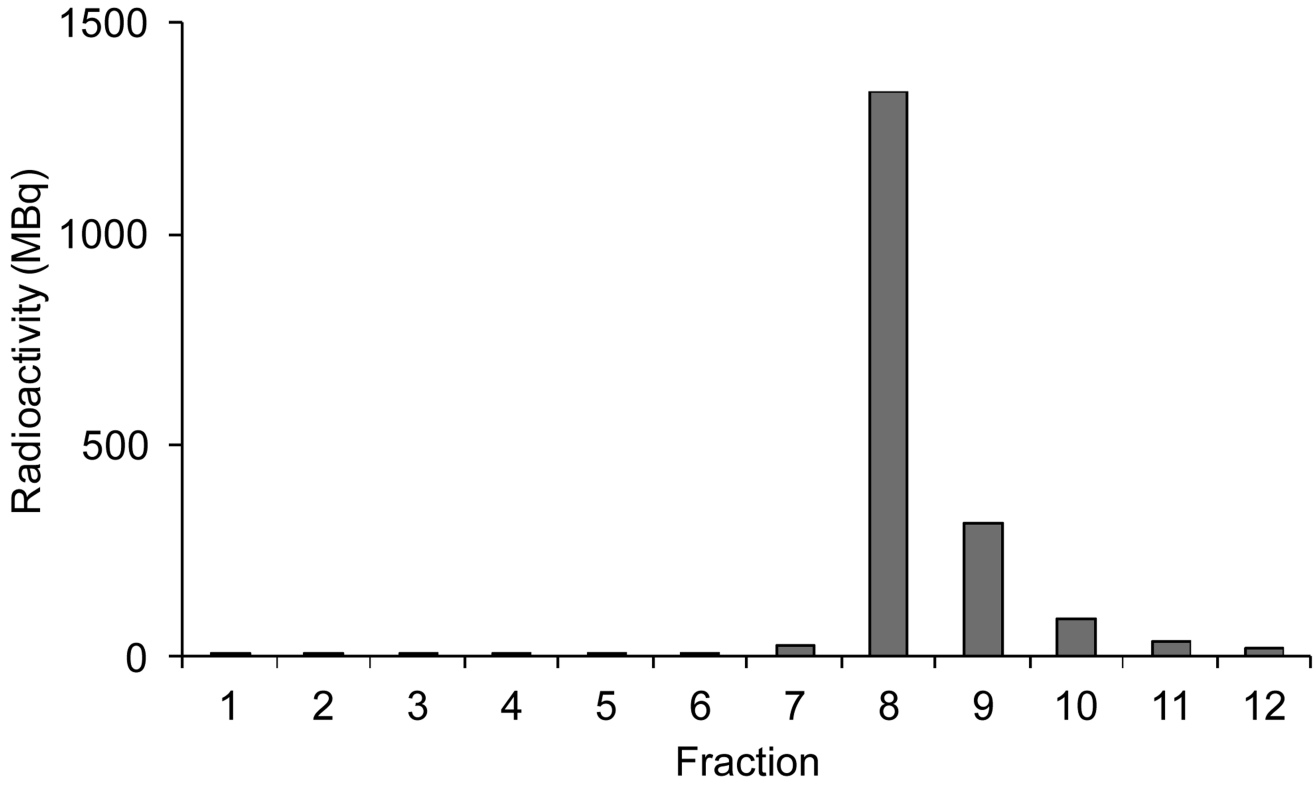


**Figure 2.**

Elution profile for $^{64}$Cu purification. Initial elution is with 5 mL 9M HCl (fraction 1), followed by 2 fractions of 3 mL and 2 mL 6M HCl respectively (fractions 2-3), then 1 mL 0.1M HCl (fraction 4) with all other fractions (5-12) being eluted with 0.5 mL 0.1M HCl.

Europe PMC Funders Author Manuscripts

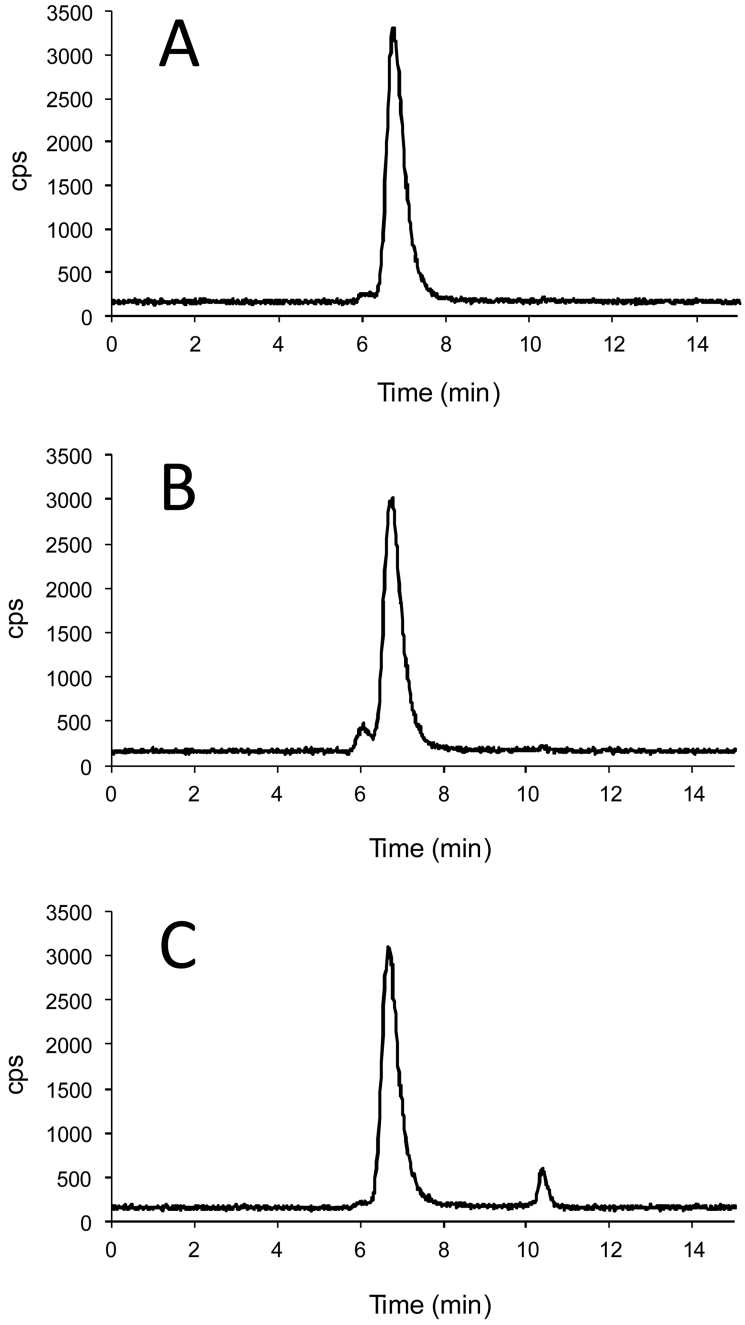


**Figure 3.**

Exemplar HPLC radiochromatograms of $^{64}$Cu labeled Rituximab conjugated with different bifunctional chelators (A) *p*-SCN-Bn-NOTA (B) *p*-SCN-Bn-PCTA (C) *p*-SCN-Bn-DTPA. NOTA- and PCTA-Rituximab show very high radiolabeling efficiency while DTPA-Rituximab shows a significant level of $^{64}$Cu impurities. The level of antibody aggregates (the peak eluting at 6 min, prior to the antibody peak) was higher for PCTA-Rituximab compared with the other immunoconjugates. Similar data acquired for the other three bifunctional chelator conjugates are shown in supplementary data.

Europe PMC Funders Author Manuscripts

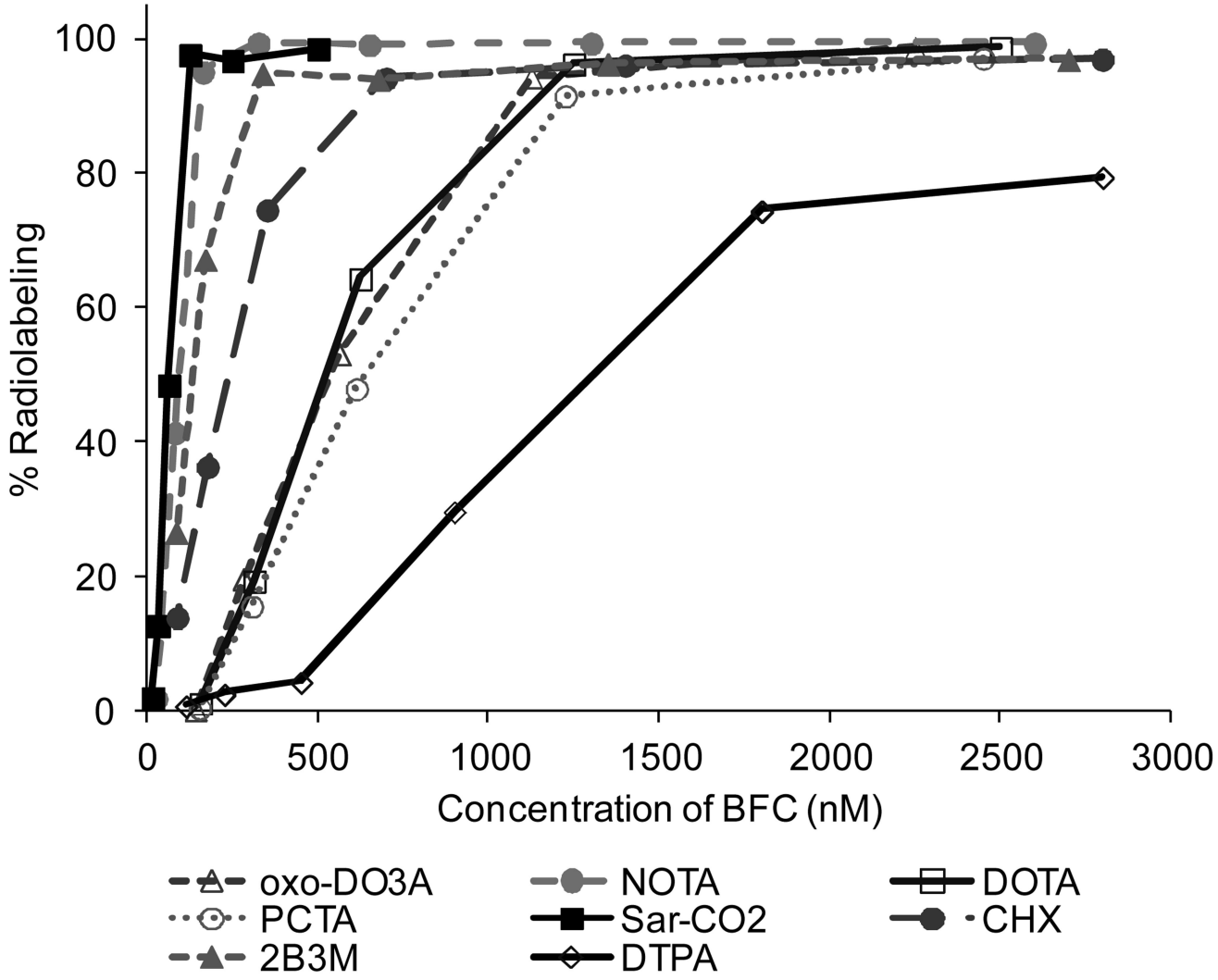


**Figure 4.**

Radiolabeling efficiency of immunoconjugates under increasingly dilute conditions expressed as % labeling efficiency against effective concentration of bifunctional chelator

Europe PMC Funders Author Manuscripts

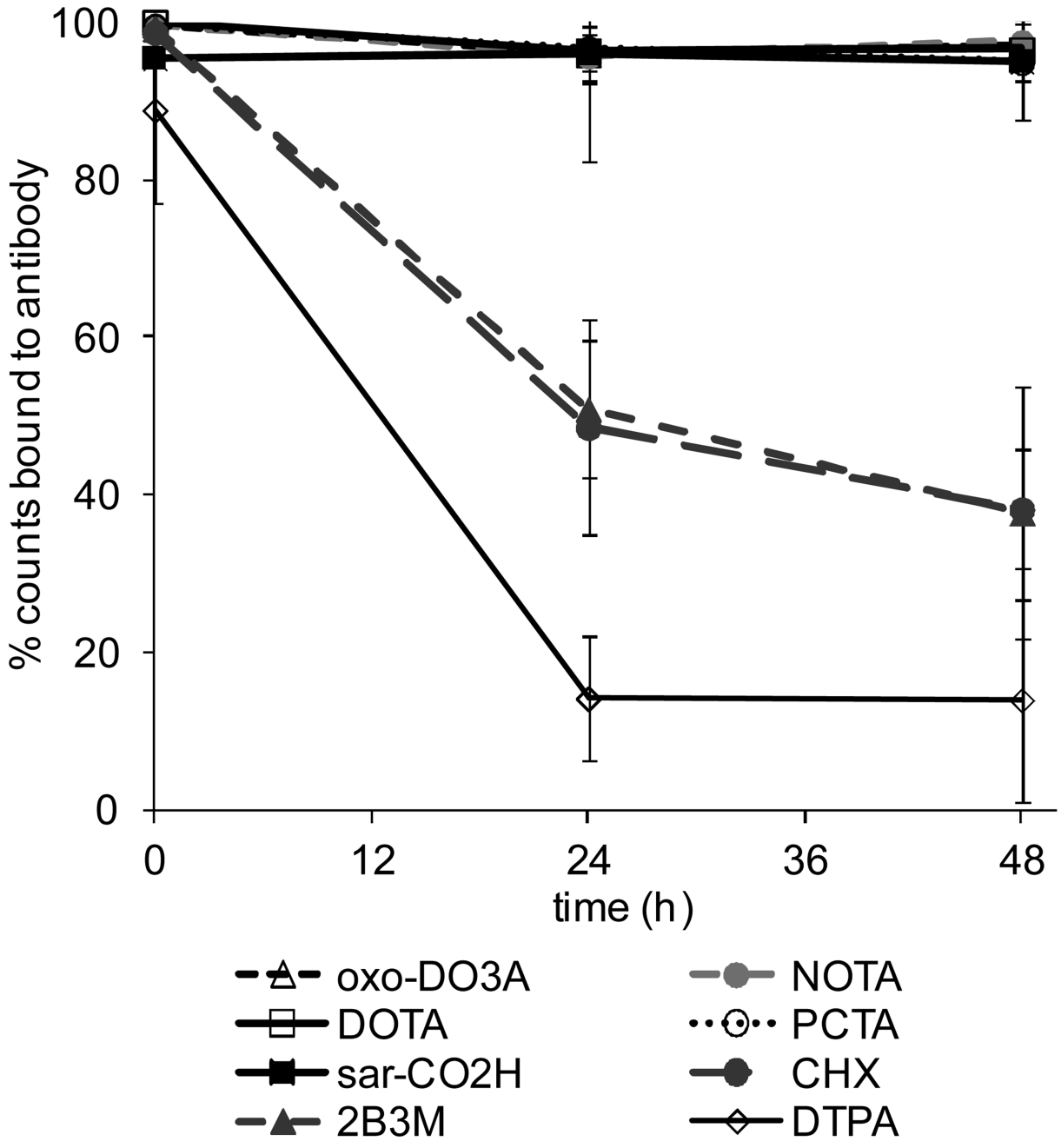


**Figure 5.**
Serum stability of $^{64}$Cu-Rituximab immunoconjugates at 37°C over 48 h (mean ± SD, n = 3) determined by size exclusion radiochromatography.

Europe PMC Funders Author Manuscripts

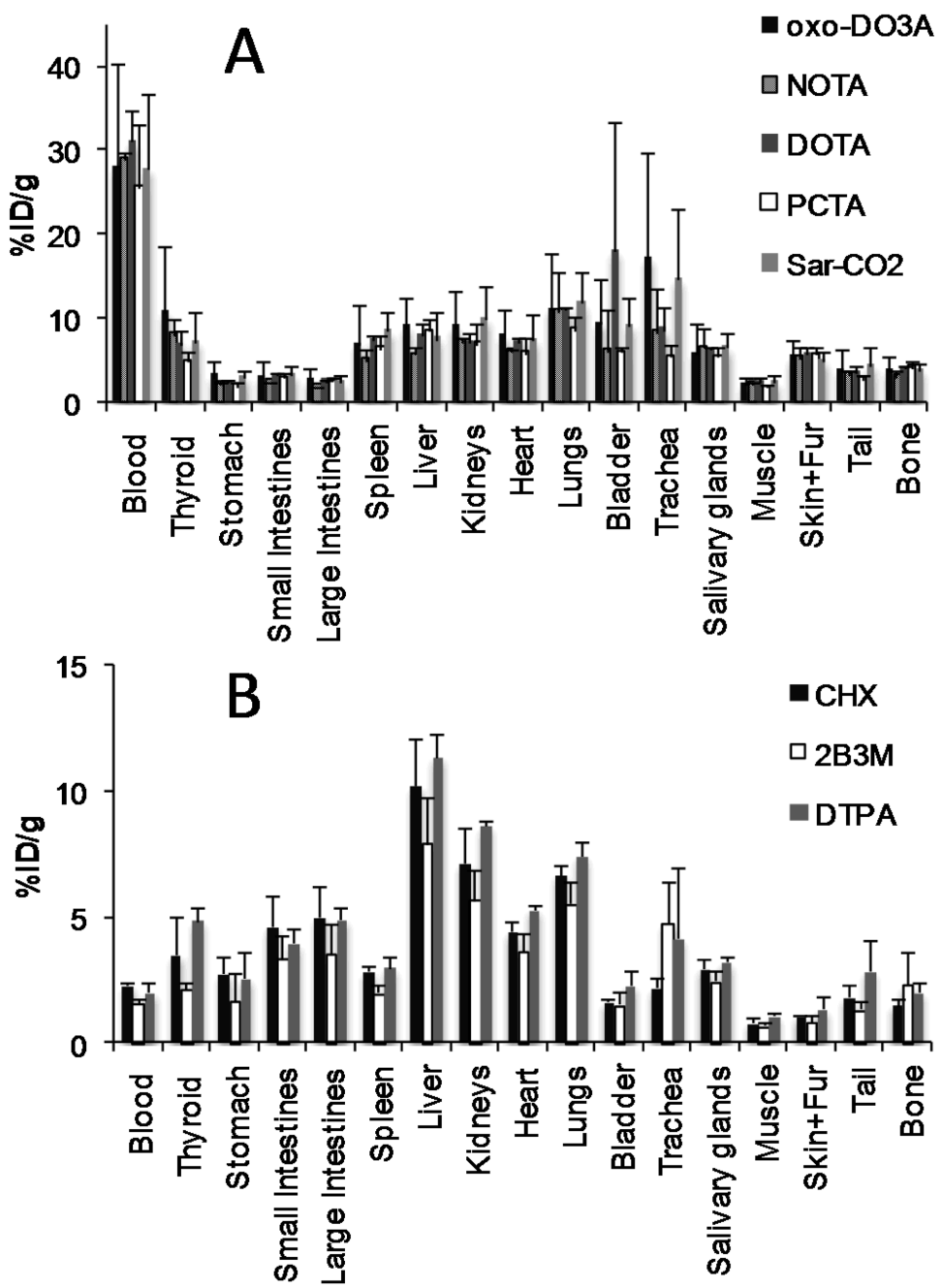


**Figure 6.**

Biodistribution of $^{64}$Cu-Rituximab-immunoconjugates in normal female Balb/C mice at 48 h post injection. The biodistribution patterns fall into two distinct groups, those containing macrocyclic chelators (A) and those containing DTPA derivatives (B).

Europe PMC Funders Author Manuscripts

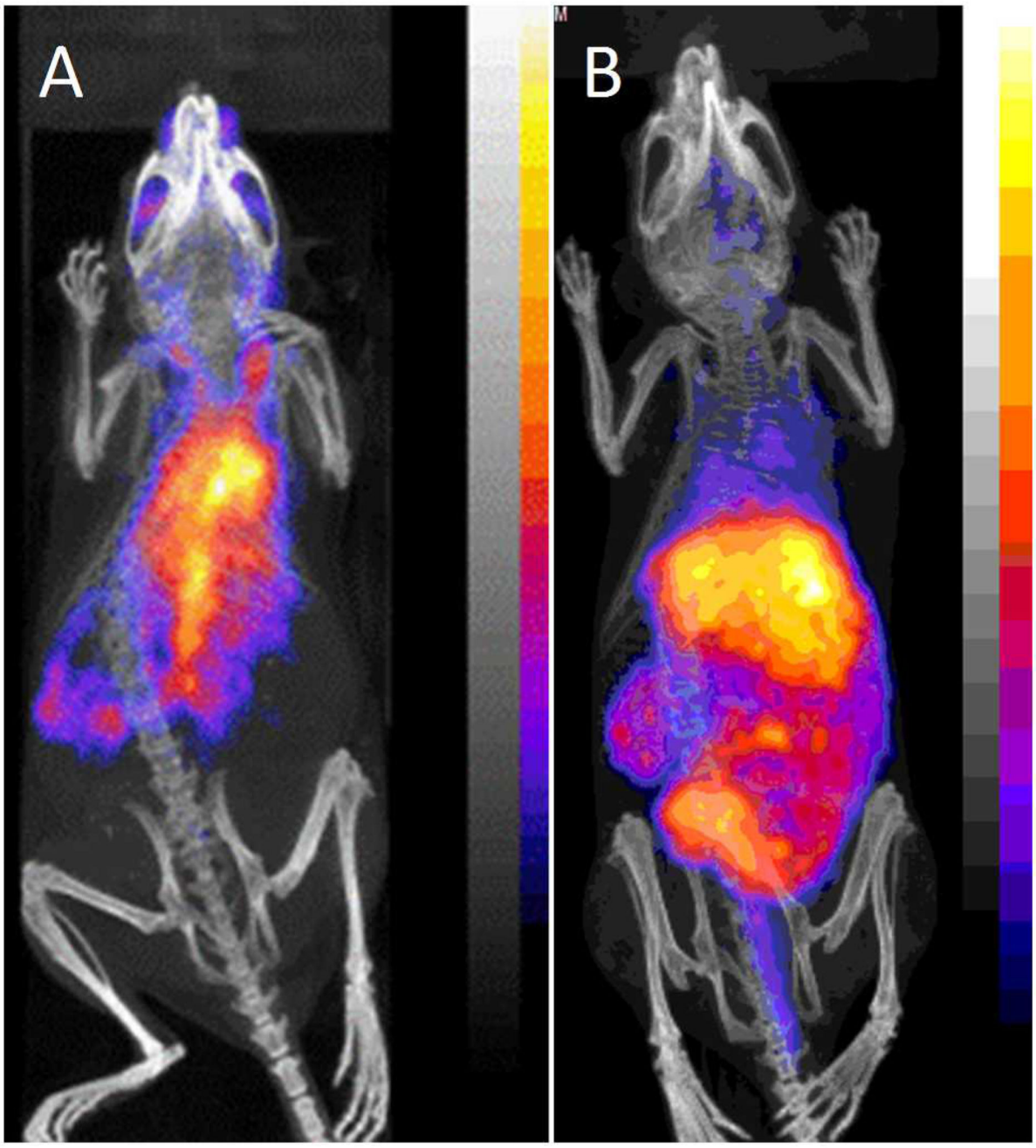


**Figure 7.**

PET/CT images (maximum intensity projection) of Balb/C mice 24 h post injection with $^{64}$Cu-Rituximab-immunoconjugates. (A) $^{64}$Cu-Sar-CO-Rituximab and (B) $^{64}$Cu-DTPA-Rituximab given as examples of macrocycle containing immunoconjugates (A, showing predominantly blood pool activity) and ,immunoconjugates containing DTPA derivatives (B, showing predominantly liver and gut activity). Corresponding images for the other chelators tested are presented in supplementary data.

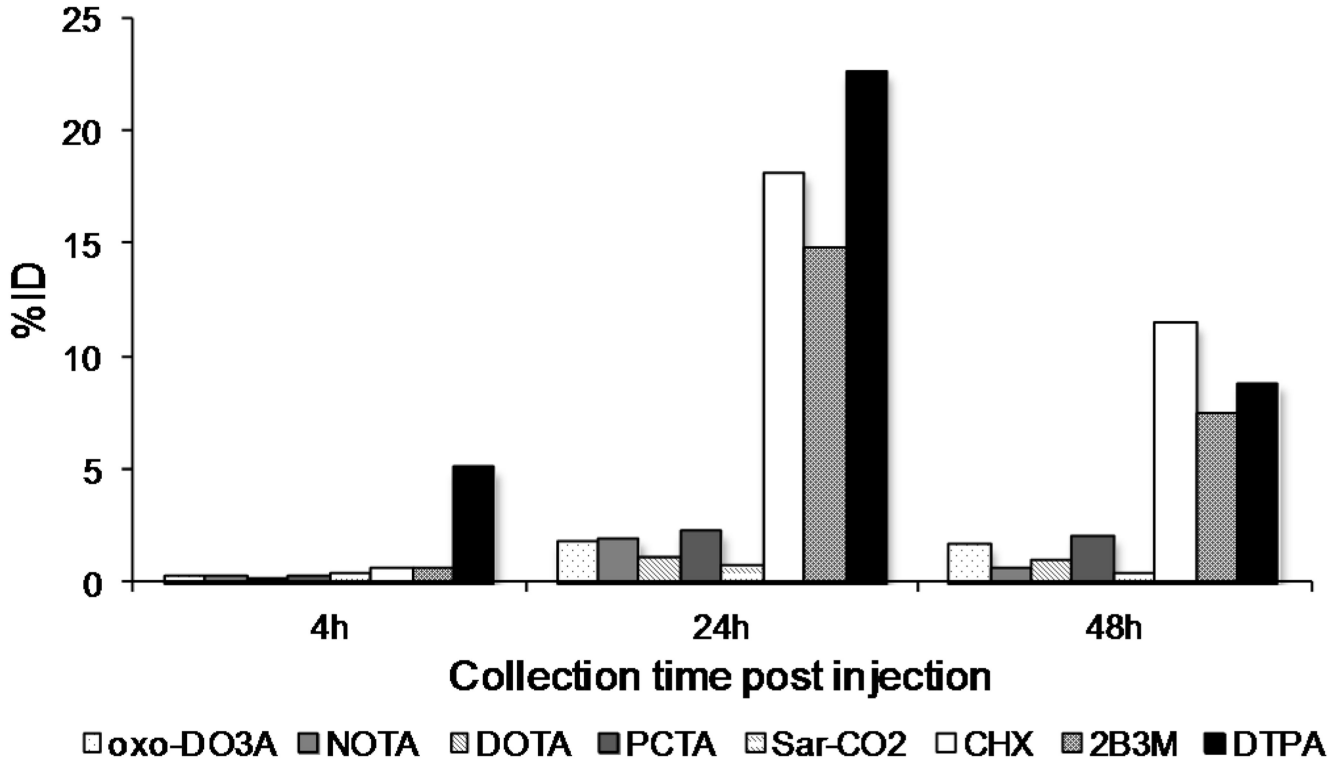


**Figure 8.**

Radioactivity (%ID) in the feces of normal female Balb/C mice at 4, 24 and 48 h post injection with $^{64}$Cu-Rituximab-immunoconjugates.

Europe PMC Funders Author Manuscripts

Europe PMC Funders Author Manuscripts

**Table 1**

Average number of bifunctional chelators per antibody molecule (±SD, n=4)

| Bifunctional chelator | Average number of chelators per antibody |
|---|---|
| *p*-SCN-Bn-DOTA | 5.0 ± 0.3 |
| *p*-SCN-Bn-NOTA | 5.2 ± 0.2 |
| *p*-SCN-Bn-oxo-DO3A | 4.5 ± 0.6 |
| *p*-SCN-Bn-PCTA | 4.9 ± 1.2 |
| Sar-$CO_2H$ | 0.5 ± 0.1 |
| *p*-SCN-Bn-DTPA | 3.6 ± 1.0 |
| CHX-A”-DTPA | 5.6 ± 0.5 |
| 2B3M-ITC-DTPA | 5.4 ± 0.5 |